Title: Contrasting growth responses in lamina and petiole during neighbor detection depend on differential auxin responsiveness rather than different auxin levels.

Authors: de Wit M, Ljung K, Fankhauser C

Journal: The New phytologist

Year: 2015 Oct

Volume: 208

Issue: 1

Pages: 198-209

DOI: 10.1111/nph.13449

New Phytologist

Contrasting growth responses in lamina and petiole during neighbor detection depend on differential auxin responsiveness rather than different auxin levels

Journal:	*New Phytologist*
Manuscript ID:	NPH-MS-2014-18667.R2
Manuscript Type:	MS - Regular Manuscript
Date Submitted by the Author:	n/a
Complete List of Authors:	de Wit, Mieke; University of Lausanne, Center for Integrative Genomics Ljung, Karin; Swedish University of Agricultural Sciences, Forest Genetics and Plant Physiology; Fankhauser, Christian; University of Lausanne, Center for Integrative Genomics;
Key Words:	neighbor detection, shade avoidance response, auxin, PIF, leaf growth, XTH

Title:

Contrasting growth responses in lamina and petiole during neighbor detection depend on differential auxin responsiveness rather than different auxin levels

Authors:

Mieke de Wit[1], Karin Ljung[2], Christian Fankhauser[1,3]

Author affiliations:

[1] Center for Integrative Genomics, Faculty of Biology and Medicine, University of Lausanne, CH-1015 Lausanne, Switzerland

[2] Umeå Plant Science Centre, Department of Forest Genetics and Plant Physiology, Swedish University of Agricultural Sciences, SE-901 83, Umeå, Sweden

[3] Corresponding author: christian.fankhauser@unil.ch, +41.21.692.39.41

Total word count main body: 6111
Summary: 183
Introduction: 1497
Material and Methods: 567
Results: 1944
Discussion: 1762
Acknowledgements: 151

Figures: 6
Supplemental Figures: 9
Supplemental Table: 1

Contrasting growth responses in lamina and petiole during neighbor detection depend on differential auxin responsiveness rather than different auxin levels

SUMMARY

- Foliar shade triggers rapid growth of specific structures that facilitate access of the plant to direct sunlight. In leaves of many plant species this growth response is complex because while shade triggers elongation of petioles it reduces growth of the lamina. How the same external cue leads to these contrasting growth responses in different parts of the leaf is not understood.
- Using mutant analysis, pharmacological treatment and gene expression analyses we investigated the role of PHYTOCHROME INTERACTING FACTOR (PIF)7 and the growth promoting hormone auxin in these contrasting leaf growth responses.
- Both petiole elongation and lamina growth reduction depend on PIF7. Induction of auxin production is both necessary and sufficient to induce opposite growth responses in petioles versus lamina. However, these contrasting growth responses are not due to different auxin concentrations in both leaf parts.
- Our work suggests that a transient rise in auxin levels triggers tissue-specific growth responses in different leaf parts. We provide evidence suggesting that this may be due to different sensitivity to auxin in the petiole versus the blade and to tissue-specific gene expression.

Keywords: neighbor detection, shade avoidance response, auxin, PIF, leaf growth, XTH

INTRODUCTION

The shade avoidance response is employed by plants upon perception of surrounding competitors in order to avoid future shade and thus maintain access to unfiltered sunlight. In Arabidopsis (*Arabidopsis thaliana*), this growth response consists of hypocotyl elongation in seedlings and of elevation (hyponasty) and

elongation of leaf petioles in older plants, which places the light capturing tissues in a higher position in anticipation of shade (Franklin, 2008; Casal, 2012). On the other hand, the growth rate of cotyledons and leaf lamina can decline upon neighbor detection (McLaren & Smith, 1978; Nagatani et al., 1991; Kozuka et al., 2010). Perception of a shade signal consequently leads to contrasting growth responses in different parts of the leaf.

Proximate neighbors are sensed through changes in light quality, mainly through a reduction in the ratio between red (R, 660-670 nm) and far-red (FR, 725-735 nm) light (Morgan & Smith, 1978; Morgan *et al.*, 1980; Ballaré *et al.*, 1990; Franklin, 2008; Casal, 2012). This decreased R:FR originates from absorption of R but reflection of FR by green plant tissues, and is therefore specifically signaling the presence of nearby plants. The R:FR is perceived through the phytochrome photoreceptors (phyA-E in Arabidopsis), of which phyB plays a predominant role in shade avoidance (McLaren & Smith, 1978; Nagatani *et al.*, 1991; Franklin *et al.*, 2003; Kozuka *et al.*, 2010). The active, FR-absorbing conformer (Pfr) of phytochrome translocates to the nucleus (Sakamoto & Nagatani, 1996) where it interacts with a class of growth-promoting basic helix-loop-helix transcription factors called PHYTOCHROME INTERACTING FACTORs (PIFs), resulting in the phosphorylation and degradation or inactivation of these PIFs (Duek & Fankhauser, 2005; Li *et al.*, 2012; Jeong & Choi, 2013; Leivar & Monte, 2014). Upon an increase in FR phytochrome shifts to the inactive, R-absorbing conformation state (Holmes & Smith, 1975; Smith & Holmes, 1977). The inactivation of phyB in low R:FR thus relieves the repression of the PIFs, which leads to their accumulation and subsequent binding to the G-box and PIF-binding E-box motifs of the promoters of shade-responsive genes (Hornitschek *et al.*, 2009; 2012; Li *et al.*, 2012; Oh *et al.*, 2012; Zhang *et al.*, 2013). PIF4, PIF5 and PIF7 play important roles in the shade avoidance response (Lorrain *et al.*, 2008; Li *et al.*, 2012), with moderate contributions of PIF1 and PIF3 (Leivar *et al.*, 2012). The PIF-mediated transcriptional response to low R:FR leads to the induction of growth-related genes and eventually to the architectural changes that make up the shade avoidance phenotype. Transcripts encoding cell wall-modifying proteins are amongst the direct PIF targets (Hornitschek *et al.*, 2009; Oh *et al.*, 2009; Hornitschek *et al.*, 2012; Oh *et al.*, 2012). Of these, the XYLOGLUCAN ENDOTRANSGLUCOSYLASE/HYDROLASES (XTHs) show increased transcription and activity during shade (Hornitschek *et al.*, 2009; Sasidharan *et al.*, 2010). XTHs can cut and ligate xyloglucan chains and play a role in cell wall rigidity (Rose *et al.*, 2002; Cosgrove, 2005). The *xth15* and *xth17* mutants have an inhibited petiole

elongation response in low R:FR, indicating their importance for the shade avoidance response (Sasidharan *et al.*, 2010).

Neighbor-induced growth responses are largely mediated by a suite of hormones, of which auxin has emerged as a major player (Gommers *et al.*, 2013; Casal, 2013; de Wit *et al.*, 2013). Auxin is perceived in the nucleus through a set of F-box TRANSPORT INHIBITOR RESPONSE/AUXIN SIGNALING F-BOX (TIR/AFB) receptors (Dharmasiri *et al.*, 2005). Auxin binding to a TIR/AFB receptor leads to degradation of AUX/IAA repressor proteins, which relieves their repression of AUXIN RESPONSE FACTOR (ARF) transcription factors (Guilfoyle & Hagen, 2007).

In low R:FR, auxin levels increase after 1h in wild-type Arabidopsis seedlings. This depends on de novo auxin synthesis through TRYPTOPHAN AMINOTRANSFERASE OF ARABIDOPSIS (TAA)1, as the *sav3/taa1* mutant fails to raise the auxin concentration in low R:FR (Tao *et al.*, 2008). The rate-limiting step in this auxin biosynthesis pathway is catalyzed by the flavin-containing monooxygenases called YUCCAs (Zhao *et al.*, 2001; Mashiguchi *et al.*, 2011; Won *et al.*, 2011). Interestingly, PIF4, PIF5 and PIF7 were shown to directly bind the promoters of *YUCCA* (*YUC*) *8* and *YUC9* (Hornitschek *et al.*, 2012; Li *et al.*, 2012), which revealed a direct link between phytochrome signaling and auxin biosynthesis. Correspondingly, auxin concentrations remain at basal levels in seedlings of the *pif4pif5* and *pif7* mutants after exposure to low R:FR (Hornitschek *et al.*, 2012; Li *et al.*, 2012). The transcriptomes of the *pif4pif5* and the *pif7* mutants consequently show miss-regulation of many auxin-related genes in response to low R:FR (Hornitschek *et al.*, 2012; Li *et al.*, 2012). The *sav3/taa1* mutant shows impaired hypocotyl elongation and leaf hyponasty, and altered leaf growth responses in low R:FR (Tao *et al.*, 2008; Moreno *et al.*, 2009), indicating that elevated auxin levels are required for the low R:FR-induced growth responses. In Arabidopsis and *Brassica rapa* seedlings auxin is mainly synthesized in the cotyledons and subsequently transported towards the hypocotyl during low R:FR treatment (Tao *et al.*, 2008; Procko *et al.*, 2014). Consistently, impaired polar auxin transport through application of the auxin transport inhibitor naphthylphtalamic acid (NPA) or mutation of the auxin export protein PINFORMED (PIN) 3 in the *pin3-3* mutant abolishes hypocotyl elongation in low R:FR (Steindler *et al.*, 1999; Tao *et al.*, 2008; Keuskamp *et al.*, 2010). NPA also inhibits petiole elongation in low R:FR, indicating that auxin transport is also required for shade avoidance in leaves (Pierik *et al.*, 2009). Apart from increasing auxin levels and flow towards expanding tissues auxin signaling is directly targeted in low R:FR,

as PIF4 and PIF5 were found to bind to the promoters of *IAA19* and *IAA29* (Hornitschek *et al.*, 2012). This is however not straightforward to interpret, as there is high redundancy and negative feedback in the auxin pathway. Plants with altered PIF levels show different sensitivity to exogenous auxin and it has been predicted that auxin sensitivity may be regulated in shade to make the tissue more receptive to auxin, especially in the case of low resource availability (Nozue *et al.*, 2011; Hersch *et al.*, 2014). We currently have poor understanding how regulation of auxin sensitivity is achieved and it may be fine-tuned at various levels (Pierre-Jerome *et al.*, 2013; Bargmann & Estelle, 2014). For shade it has been suggested that the AFB1 receptor might play a role in this, as its gene expression is induced in hypocotyls of shade-treated seedlings (Hersch *et al.*, 2014).

Most shade avoidance studies have focused on hypocotyl and petiole elongation, but whether auxin also plays a role in the reduction of lamina size in low R:FR is currently not known. In leaf primordia, neighbor detection leads to rapid reduction of cell division due to auxin-dependent degradation of cytokinin (Carabelli *et al.*, 2007). However, shade also induces lamina growth reduction in older leaves when cell proliferation is largely arrested (Donnelly *et al.*, 1999; Andriankaja *et al.*, 2012), and is thus likely to affect cell expansion as well. In end-of-day far-red, a treatment that evokes a shade avoidance-like phenotype, a large amount of auxin-responsive genes are induced in both petioles and lamina (Kozuka *et al.*, 2010). Furthermore, it has been shown that an increase of auxin levels by application of auxin or NPA (thereby increasing endogenous levels) resulted in inhibited leaf growth in Arabidopsis and common bean (*Phaseolus vulgaris)* (Keller *et al.*, 2004). It therefore seems plausible that low R:FR-induced auxin biosynthesis could play a role both in growth promotion in the petiole and in growth reduction in the lamina. The effects that auxin generates in a cell are dependent on cellular context and developmental age (Kieffer *et al.*, 2010). Furthermore, active auxin transport through export carriers leads to gradient formation and different concentrations across tissues and organs (Zazimalova *et al.*, 2010). Auxin responses are known to be concentration-dependent and can follow an optimum curve as is the case for root elongation which is promoted at low auxin levels, but inhibited at higher auxin levels (e.g. Wilson & Wilson, 1991; Evans *et al.*, 1994). A similar optimum curve has been hypothesized to exist for PIF-dependent hypocotyl elongation in response to auxin (Nozue *et al.*, 2011). Organ-specific auxin responses may thus be due to different auxin levels, a difference in auxin sensitivity or a combination of both.

Here, we investigate the contrasting growth responses of the shade avoidance leaf phenotype in Arabidopsis. Our data suggests that both petiole elongation and lamina size reduction in low R:FR are an effect of PIF7-dependent auxin production in the lamina. However, we find that overall auxin levels are not significantly different between petiole and lamina, neither in control light nor after low R:FR induction. The contrasting growth responses of petiole and lamina thus rather appear to be due to different auxin responsiveness. Although abundance of the AFB1 receptor is specifically upregulated in petioles in low R:FR, a functional role for this only became apparent in absence of auxin biosynthesis. Enhanced auxin sensitivity through receptor regulation may therefore be mainly important in limiting conditions. We hypothesize that PIF7 regulates tissue-specific growth-related genes both dependent and independent of auxin.

MATERIAL AND METHODS

Plant growth, treatments and measurements

All mutant lines are in the Col-0 background: *hfr1-101* (Fankhauser & Chory, 2000), *sav3-2* (Tao *et al.*, 2008), *tir1afb* mutants and *35S::AFB1-Myc* (Dharmasiri *et al.*, 2005), *msg2-1* (Tatematsu *et al.*, 2004), *iaa5iaa6iaa19* (Overvoorde *et al.*, 2005). The *pif4pif5pif7* mutant was obtained by crossing *pif7-1* (Leivar *et al.*, 2008) with *pif4-101pif5 (pil6-1)* (Lorrain *et al.*, 2008). Seeds were sown on soil and stratified for three days at 4°C in the dark. Plants were grown in a 16h light / 8h dark photoperiod of 220 µM m^2 s^{-1} at 20°C and 70% RH. After 14d plants were divided over two Percival Scientific Model I-66L incubators and acclimatized to 130 µmol m^{-2} s^{-1} for 24h. The next morning at ZT3 one incubator was supplemented with 45 µM m^2 s^{-1} of FR light (739 nm LEDs, Quantum Device, USA), lowering the R(640-700 nm):FR (700-760 nm) from 1.4 to 0.2, as measured by Ocean Optics USB2000+ spectrometer.

10 µM IAA (SIGMA-Aldrich), 25 µM NPA (Duchefa Biochemie), 500 µM L-Kynurenine (SIGMA-Aldrich) and 200 µM α-(phenylethyl-2-oxo)-indole-3-acetic acid (PEO-IAA, provided by H. Nozaki) solutions were freshly prepared from concentrated DMSO stocks before each application. Mock solution was similarly prepared to contain 0.1% DMSO and 0.15% Tween-20. Solutions were applied adaxially with a paintbrush, prior to the start of light treatment.

After three days of treatment the third leaf was removed from ten plants per treatment and incisions were made in the lamina to allow leaf flattening. Leaves were scanned on a flatbed scanner (600 dpi) using a uniform blue background. This

allowed automated separation from the background in Matlab (Methods S1) using the Green/Blue pixel value. Petiole base and petiole-lamina junction were selected manually. Pixels located below the petiole-lamina junction were labeled as petiole and above as lamina. Transformation of pixel coordinates to petiole length and lamina area were done using the image resolution given by the scanner.

RNA extraction and RT-qPCR

Petioles and lamina of leaf 3 were separately pooled into three biological replicates and frozen in liquid nitrogen. RNA was extracted using the Qiagen Plant RNeasy kit with on-column DNA digestion, according to the manufacturer's instructions. For each experiment, equal amounts of RNA were reverse transcribed into cDNA with Superscript II Reverse Transcriptase (Invitrogen). RT-qPCR was performed in three technical replicates for each sample (7900HT Applied Biosystems). Data was normalized against two reference genes (*YLS8, UBC*) using the Biogazelle qbase software.

IAA content and MUG assays

For IAA measurements, five biological replicates per timepoint containing 12 mg fresh weight of petioles or lamina were harvested and frozen in liquid nitrogen. 500 pg $^{13}C_6$-IAA internal standard was added to each sample before extraction and purification. Free IAA was quantified using gas chromatography – tandem mass spectrometry as described in (Andersen *et al.*, 2008) with minor modifications.

For AFB1-GUS quantification, three biological replicates consisting of petioles or lamina from ten *pAFB1::AFB1-GUS* plants were frozen in liquid nitrogen. Proteins were extracted from ground material with GUS extraction buffer (50mM $NaPO_4$, 10mM 2-ME, 10mM EDTA, 5% glycerol, 0.1% Triton-X). 10 µL of protein extract was incubated in 140 uL of MUG assay buffer (1mM 4-Methylumbelliferyl-B-D-glucuronide hydrate (SIGMA-Aldrich) in GUS extraction buffer) for 55 minutes at 37 °C. The enzyme reaction was stopped in 2M $NaCO_3$ and fluorescence measurements were done in duplicate in a Tecan Saphire^2 platereader. Protein concentrations were determined in duplicate at OD_{595} using the Biorad Protein Assay.

RESULTS

Low R:FR induces contrasting leaf responses dependent on PIF7

To study responses of lamina and petiole during neighbor detection we subjected two-week-old plants to several days of low R:FR. In agreement with previous studies (McLaren & Smith, 1978; Nagatani *et al.*, 1991; Reed *et al.*, 1993; Kozuka *et al.*, 2010), leaves of low R:FR-treated plants showed a reduced lamina size and elongated petioles as compared to leaves of plants in control white light (high R:FR), which was also reflected in their biomass allocation (Fig. S1a-d). For further experiments we measured leaf 3, which reliably shows both leaf responses after three days of low R:FR treatment (Fig. 1a,b). In this leaf, the gene expression kinetics of typical shade avoidance markers (as shown for *PIL1* in Fig. 1c) were largely similar for lamina and petiole. Low R:FR-induced expression of the negative shade avoidance regulator *HFR1* was higher in lamina than in petioles (Fig. S2a). The lamina response in low R:FR was however not affected in the *hfr1* mutant suggesting that in our growth conditions HFR1 does not play a limiting role in the reduced lamina growth during shade avoidance (Fig. S2b,c).

In seedlings, PIF4, PIF5 and PIF7 are important regulators of the shade avoidance response (Lorrain *et al.*, 2008; Li *et al.*, 2012) and we therefore tested petiole length and lamina size in *pif* mutants after three days of low R:FR. *pif7* had a reduced petiole response in low R:FR (138% (1.8 mm) length increase vs. 153% (3.0 mm) in the wild-type), while the smaller *pif4pif5* petioles showed a strong elongation response (166% (2.3 mm) length increase) (Fig. 1d, S3a). Similarly, lamina size was not reduced in *pif7* after low R:FR treatment, while *pif4pif5* still showed a tendency towards reduced lamina area (p=0.05, Fig. 1e, S3b). Although *pif4pif5pif7* plants were smaller than *pif7* plants, they only showed a slightly greater inhibition in petiole elongation as *pif7* (130% (1.0 mm)) and no lamina size reduction in response to low R:FR (Fig. 1e,d, S3). This indicates that among the tested PIFs, PIF7 plays the predominant role in regulating these leaf growth traits in response to low R:FR conditions.

Auxin biosynthesis is required and sufficient to induce both leaf responses

The *pif7* mutant has impaired *YUCCA* activation in low R:FR-treated seedlings (Li *et al.*, 2012) and induced auxin production through the TAA1-YUCCA pathway is an important step during shade avoidance in seedlings (Tao *et al.*, 2008). We therefore tested whether this also plays a role in the lamina and petiole responses of juvenile leaves. All four *YUCCA* genes that were reported to be shade-induced in seedlings showed increased expression in the lamina after 2 hours of low R:FR (Fig. 2a-c). In contrast, only *YUC9,* which showed the highest shade-induced expression in the lamina, also showed increased expression in the petiole. Moreover, the magnitude of

induced *YUC9* expression by low R:FR was six times lower in the petiole than in the lamina (Fig. 2d). *YUC8* expression was dramatically reduced in *pif7* lamina compared to the wild type (Fig. 2e). Shade-regulated *YUCCA* expression correlated with an increase in auxin levels in wild-type lamina after 2h of low R:FR, while the auxin concentration in *pif7* lamina remained similar to control light conditions (Fig. 2f), indicating that low R:FR-induced auxin biosynthesis in leaves is PIF7-dependent. Interestingly, the *pif7* shade avoidance phenotype resembles that of the *sav3/taa1* mutant (Fig. 2e, S4a,b), which lacks an induced auxin burst in low R:FR (Tao *et al.*, 2008). The impaired petiole and lamina responses of *pif7* could thus be due to failure to induce auxin biosynthesis upon neighbor detection.

The *YUCCA* expression pattern suggests that low R:FR-induced auxin production mainly takes place in the lamina (Fig. 2). Interestingly, the auxin signaling marker *DR5::GUS* is induced at the leaf margins in low R:FR (Fig. S4c), which in cotyledons coincides with the site of *TAA1* expression (Tao *et al.*, 2008). We therefore hypothesized that by analogy with seedlings most auxin would be produced in the leaf lamina and would subsequently be transported into the petiole. It has been shown previously that the auxin transport inhibitor NPA can inhibit low R:FR-induced petiole elongation (Pierik *et al.*, 2009a). Application of NPA to the lamina-petiole junction was sufficient to completely inhibit the petiole response to low R:FR (Fig. S4d), suggesting that auxin flow from lamina to petiole is required. Expression of the gene coding for the auxin efflux carrier PIN3 was upregulated both in lamina and petioles in the first few hours of low R:FR treatment (Fig. S4e), which may facilitate enhanced basipetal auxin transport upon neighbor detection.

To test whether increased auxin biosynthesis in the lamina could account for the leaf responses induced by low R:FR, we applied IAA to the adaxial side of the leaf lamina and especially at the leaf margins. In comparison to mock-treated plants, application of various concentrations of IAA to the lamina induced petiole elongation and reduced growth of the lamina (Fig. 3a,b, Fig. S5a,b). This shows that increased auxin levels in the lamina can lead to both leaf phenotypes as observed in low R:FR. Moreover, the *pif7* and *pif4pif5pif7* mutants also responded to IAA application, suggesting that their reduced leaf phenotypes in low R:FR is mainly due to impaired auxin biosynthesis (Fig. S5c,d). Correspondingly, application of NPA to the lamina-petiole junction, which should increase endogenous auxin levels in the lamina and inhibit auxin transport to the petiole, reduced both petiole and lamina growth (Fig. 3c,d). Reduction of basal auxin levels through application of the biosynthesis inhibitor L-Kynurenine led to increased lamina size but had no effect on petiole growth (Fig. 3e,f), suggesting that basal auxin levels in control conditions are indeed sub-optimal

for lamina growth. Together, these results correspond to a model in which PIF7-dependent auxin production takes place mainly in the lamina leading to lamina growth reduction and in which auxin is subsequently transported to the petiole leading to enhanced petiole growth.

Contrasting leaf responses are not due to different auxin concentrations

Auxin responses can be concentration-dependent (Wilson & Wilson, 1991; Evans *et al.*, 1994) and we therefore asked whether the contrasting growth responses of lamina and petiole to low R:FR could be due to a different auxin concentration in both leaf parts. If the lamina is indeed the site of auxin production then auxin levels might be relatively high in lamina compared to petioles. In agreement with this basal expression levels (plants grown in high R:FR) of both an auxin biosynthesis (*YUC8*) and an auxin responsive (*IAA29*) gene were higher in lamina compared to petioles (Fig. 4a,b). Thus, a further increase in auxin production upon low R:FR perception may shift the auxin optimum curve further towards growth reduction in the lamina, while auxin transported to the petiole may increase the auxin concentration further within the lower growth-stimulating range. To test this, we measured overall auxin levels in entire lamina and petioles after 0.5h, 1h, 2h and 24.5h of low R:FR treatment. Based on previously published seedling data and on the expression of the two highest induced *YUCCAs* in leaves (Fig. 4c,S6) we expected auxin levels to rise within this timeframe in lamina. As shown in Fig. 4d and e, auxin concentration indeed increased within 2h of low R:FR treatment and were back to basal levels after 24h. The kinetics were similar for petioles and lamina, and despite the early timepoints no indication that auxin levels first increase in the lamina could be observed. Interestingly, after 2h of low R:FR the auxin concentration reaches very similar levels in both leaf parts. These concentration data indicate that the contrasting growth responses of lamina and petiole to auxin are not due to a global concentration difference.

Auxin responsiveness in low R:FR-treated petioles

The different responses of lamina and petiole to increased auxin levels may alternatively be due to a difference in sensitivity to auxin, which could be under regulation of light signals. One way in which auxin sensitivity could be regulated is at the level of receptor abundance. In seedlings gene expression of the AFB1 receptor was shown to be hypocotyl-specific, which may suggest that auxin sensitivity is locally enhanced and could contribute to the shade-induced elongation response (Hersch *et al.*, 2014). Of the four *TIR/AFBs* tested, only *AFB1* was upregulated in low

R:FR, both in petioles and lamina (Fig. 5a,b, S7). Interestingly, *AFB1* was also upregulated in petioles of *pif7* (Fig. 5b). If induced *AFB1* expression indeed leads to enhanced sensitivity, this might explain why the petiole response in low R:FR is not completely abolished in this mutant despite the lack of induced auxin levels. Overall, AFB1 protein levels in control light conditions were higher in petioles than in lamina (Fig. 5c), as measured by GUS activity of AFB1-GUS protein under the expression of the AFB1 promoter (Parry *et al.*, 2009). Furthermore, although *AFB1* expression levels were induced in both leaf parts in low R:FR, AFB1-GUS levels were increased only in petioles upon low R:FR treatment (Fig. 5c). Such a difference in receptor levels may play a role in the different responsiveness of the two leaf parts to auxin. Nevertheless, a role for AFB1 in shade-induced petiole elongation could not be deduced from higher-order receptor mutants lacking AFB1 or a *35S::AFB1* over-expression line (Fig. S8), which all showed a normal elongation response in low R:FR (Fig. 5d). As Aux/IAAs can act as co-receptors (Calderon-Villalobos *et al.*, 2012; Havens *et al.*, 2012) and IAA6 and IAA19 is induced in low R:FR (Kozuka *et al.*, 2010; Hornitschek *et al.*, 2012), we also tested the *iaa5iaa6iaa19* triple mutant and the dominant IAA19 mutant *msg2* (Fig. S8). Neither of these lines was affected in low R:FR-induced petiole elongation. The lack of a phenotype in the receptor- and *iaa* mutants could however be due to redundancy with the other TIR/AFBs or Aux/IAAs and/or to the fact that auxin production should still be induced in these mutants upon low R:FR perception, which could compensate a reduced sensitivity. Indeed, application of the auxin antagonist PEO-IAA that binds to the TIR/AFBs only reduced low R:FR-induced petiole elongation in the wild type at a high concentration (Fig. 5e), but led to a significantly decreased petiole response at a lower concentration in mutants with impaired induction of auxin biosynthesis (Fig. 5f,g). It is thus possible that regulation of auxin sensitivity through the TIR/AFBs may play a role in low R:FR-induced petiole elongation mainly when auxin levels are low. A similar role for auxin sensitivity was recently predicted for low R:FR-induced hypocotyl elongation in low light conditions, in which seedlings have low auxin levels (Hersch *et al.*, 2014) .

Leaf part-specific PIF7 targets

Ultimately, PIF7 should confer tissue-specific responses by regulating specific gene targets, either directly through binding to their promoters, or indirectly through auxin-mediated changes in gene expression. The cell wall-modifying proteins of the XTH family have been implicated in shade avoidance previously (Hornitschek *et al.*, 2009; Kozuka *et al.*, 2010; Sasidharan *et al.*, 2010). Moreover, the expression of some

members of the *XTH* gene family is regulated by auxin while this is not the case for others (Yokoyama & Nishitani, 2001; Nemhauser *et al.*, 2006; Chapman *et al.*, 2012). We therefore decided to analyze the expression of members of the XTH family in the petiole and the lamina of shade treated seedlings. Interestingly, *XTH15/XTR7* and *XTH19* showed a leaf part-specific expression pattern, with *XTH15* being predominantly upregulated in the lamina and *XTH19* being mainly induced in the petiole (Fig. 6a,b). This leaf part-specific induction of the *XTH*s in low R:FR was strongly reduced in the *pif7* mutant (Fig. 6c,d) while *PIF7* levels were high in both petioles and lamina (Fig. S9), which may be due to a different auxin-mediated transcriptional readout in the lamina versus the petiole.

DISCUSSION

Specificity in auxin responses depends both on auxin concentration and auxin responsiveness (Del Bianco & Kepinski, 2011). In this work, we showed that both contrasting growth responses of petiole and lamina in low R:FR are auxin-mediated (Figs. 1-3), but that auxin levels are very similar in the two leaf parts both in control light and in low R:FR (Fig. 4). This suggests that the opposite responses of petioles and lamina are not due to a difference in auxin concentration, although as we have analyzed entire petioles and lamina it remains possible that there is a concentration difference in specific cells that mediate the growth responses. Another interesting feature of the concentration measurements is that after 24h of low R:FR auxin levels were back to the base values despite elevated levels of *YUC8* and *YUC9* at this timepoint (Fig. 4, S3), which was shown previously in seedlings (Bou-Torrent *et al.*, 2014). This implies that shade-induced auxin biosynthesis is transient or alternatively the transient nature of increased auxin levels may be regulated through irreversible degradation of auxin to inactive catabolites (Pencik *et al.*, 2013). This is somewhat surprising considering the importance of auxin biosynthesis for the shade avoidance response (Tao *et al.*, 2008) and the fact that low R:FR-mediated growth of petiole and lamina continues over multiple days (Fig. S1). The concentration kinetics may point towards a role for auxin biosynthesis especially during the first hours of shade avoidance signaling, in which auxin is required for reprogramming of developmental processes until a new growth homeostasis is reached. However, our gene expression analysis suggests that there may be additional smaller peaks of auxin production in low R:FR-grown plants as both *YUC8* and *YUC9* expression levels

show small rises in expression levels on days two and three of the shade treatment (Fig. 4, S6).

Our data suggests that in juvenile leaves low R:FR-induced auxin synthesis mainly takes place in the lamina (Fig. 2, S4d), although this was not apparent in our concentration measurements (Fig. 4). If the lamina is indeed the source of rising auxin levels in the petiole in low R:FR, the newly synthesized auxin would therefore have to be immediately transported away to the petiole by means of polar transport or the phloem. Speed of rootward auxin transport has been determined to be 7-8 mm h^{-1} for the Arabidopsis inflorescence, but may vary between different organs (Kramer *et al.*, 2011). Such a transport rate could be sufficient to transport auxin from the leaf margins to the petiole in 15-day-old plants within the measured timepoints and may even be increased in shade. The PIN3 export carrier was shown to adopt a more lateral position in low R:FR-treated hypocotyls (Keuskamp *et al.*, 2010) and *PIN3* was upregulated in both petioles and lamina in low R:FR (Fig. S4e), which may result in increased protein abundance and enhanced auxin export. How far auxin can subsequently travel after excretion into the apoplast depends on the auxin influx carriers, fraction of molecules that becomes protonated and thus becomes membrane permeable, permeability of the cell membranes and cell wall thickness (Kramer, 2006; Swarup & Péret, 2012). Apoplastic acidification happens within minutes of the onset of a shade signal in Arabidopsis petioles (Sasidharan *et al.*, 2010), which will increase the protonated fraction of auxin molecules and consequently diffusion into cells. It may thus be possible that the increased auxin concentration in petioles is due to transport from the lamina. Alternatively, low R:FR also induces auxin production in petioles. Although the *YUCCA*s were predominantly upregulated in the lamina, *YUC9* was also induced in the petioles after 2h of low R:FR (Fig. 2). It has been shown in ten-day-old Arabidopsis seedlings that all plant parts including hypocotyls, cotyledons, roots and leaves have the capacity to synthesize auxin, but this has not been specified for lamina and petioles separately (Ljung *et al.*, 2001). It was shown recently that cotyledon-specific overexpression of *YUC3* in a quintuple *yuc* mutant background leads to an auxin overexpression phenotype in both cotyledons and hypocotyls but not in roots (Chen *et al.*, 2014), indicating that local auxin production can be required for certain responses.

As overall auxin concentration was similar between petioles and lamina while their growth response to IAA application is opposite, it is likely that their contrasting growth in response to low R:FR-induced auxin production are due to a difference in auxin

sensitivity. Different responsiveness to auxin could be brought about by a context-specific difference in abundance of auxin signaling components, such as receptors, Aux/IAAs and/or ARFs. Regulation of environmental responses through altered expression levels of TIR/AFB receptors has been reported previously for pathogen defense and root responses to nutrient availability (Navarro *et al.*, 2006; Perez-Torres *et al.*, 2008; Vidal *et al.*, 2013), and *AFB1* expression shows hypocotyl-specific induction in low R:FR (Hersch *et al.*, 2014). In juvenile leaves, *AFB1* expression was upregulated both in petioles and lamina (Fig. 5a,b), but AFB1 protein levels were increased by low R:FR specifically in petioles (Fig. 5c). This however seems to play a minor role in our experimental conditions as *tir/afb* mutants showed a normal petiole response in low R:FR and PEO-IAA treatment only affected the petiole response in Col-0 at high concentration (Fig. 5d,e). It was recently predicted by a computational model of low R:FR-dependent hypocotyl elongation that enhanced auxin sensitivity may be especially important when there is a low auxin signal (Hersch *et al.*, 2014). Correspondingly, we found that a PEO-IAA concentration that had no effect on the wild type did inhibit petiole elongation in the *sav3* and *pif7* mutants, of which the latter also shows increased *AFB1* expression in low R:FR (Fig. 5). Regulation of the AFB1 auxin receptor may thus be an important mechanism to ensure elongation responses in shade particularly when overall IAA levels are low. Upregulation of AFB1 receptor during neighbor detection, such as in our experimental conditions, may be important to anticipate future shading events. The Aux/IAAs and ARFs are other components of the auxin pathway that may confer specificity. End-of-day-FR was previously reported to lead to higher induction of *IAA19* and *IAA6* in petioles than in lamina (Kozuka *et al.*, 2010). The Aux/IAAs act as co-receptors and different combinations of TIR/AFB – Aux/IAA have different auxin-binding affinities (Calderon-Villalobos *et al.*, 2012; Havens *et al.*, 2012). Abundance of different IAAs could thus determine the sensitivity of a tissue. Although we found that low R:FR-induced petiole elongation was not affected in the *iaa5iaa6iaa19* and *msg2* mutants (Fig. S8), it would be informative to study different combinations of higher order *tir/afb* – *aux/iaa* mutants to unravel a putative role of auxin receptor complexes in the shade avoidance response. Furthermore, different IAAs may interact with different ARFs (Vernoux *et al.*, 2011) and thus affect transcription of different targets. Furthermore, ARFs are known to show distinct spatial and developmental expression patterns (Rademacher *et al.*, 2011) and may be leaf part-specific. Finally, a specific auxin response may depend on tissue-specific chromatin structure, which may make certain auxin-responsive genes more or less accessible for the transcriptional machinery (Widman *et al.*, 2014).

Here, we showed that two different genes of the *XTH* family, *XTH15* and *XTH19,* show a leaf part-specific expression pattern in low R:FR which was reduced in the *pif7* mutant (Fig. 6). *XTH15* was previously shown to be upregulated in petioles after 24h of low R:FR treatment (Sasidharan *et al.*, 2010). We found a similarly small upregulation in petioles after 24h (1.8 fold), but a much more significant upregulation in lamina at earlier timepoints (23 fold after 4h of low R:FR). XTHs are cell wall-modifying enzymes that can play a role in both cell wall loosening and cell wall strengthening (Takeda *et al.*, 2002; Cosgrove, 2005; Mellerowicz *et al.*, 2008). Whether the induction of *XTH15* and *XTH19* depends on transcriptional activity of PIF7 itself or on PIF7-dependent auxin biosynthesis cannot be distinguished from our data. Previously published data shows that *XTH15/XTR7* is a target of PIF1, PIF3, PIF4 and PIF5 and that its expression is reduced in the *pif4pif5* mutant, while *XTH19* does not appear in ChIP-seq data of PIF targets (Hornitschek *et al.*, 2009; Oh *et al.*, 2009; Hornitschek *et al.*, 2012; Oh *et al.*, 2012; Zhang *et al.*, 2013). On the other hand, expression of *XTH19* is auxin responsive (Yokoyama & Nishitani, 2001; Vissenberg, 2005; Nemhauser *et al.*, 2006; Chapman *et al.*, 2012; Pitaksaringkarn *et al.*, 2014), while *XTH15* does not appear to be auxin inducible (Yokoyama & Nishitani, 2001; Nemhauser *et al.*, 2006; Chapman *et al.*, 2012). Hence, while shade-induced *XTH15* expression in the lamina may be directly mediated by the PIFs, the expression of *XTH19* in the petiole may rather be due to the PIF7-mediated increase in auxin levels. Indirect evidence for this hypothesis comes from studies investigating shade avoidance with other light treatments (low blue or green shade). In response to attenuated blue light, a treatment that also leads to PIF-mediated shade responses (Keller *et al.*, 2011), induction of *XTH15* was not inhibited by PEO-IAA (Keuskamp *et al.*, 2011) and neither was its green shade induction inhibited by NPA (Sasidharan *et al.*, 2014). *XTH19* induction however was reduced in green shade after NPA treatment and in the TAA1-mutant *wei8* (Sasidharan *et al.*, 2014), showing that *XTH19* expression is auxin-dependent in a shade context. As it was recently shown that PIFs and ARFs may interact to jointly regulate target genes (Oh *et al.*, 2014), the expression of some shade-induced genes might also depend both on PIFs and auxin signaling components. Hence, different combinations of PIF and auxin-mediated transcriptional readouts may underlie the tissue-specific growth responses in the leaf.

Besides tissue-specific regulation of growth regulators such as the *XTH*s, there may be tissue-specific hormonal interactions that determine different organ responses. In

young leaf primordia shade-induced auxin mediates a cytokinin-mediated reduction in cell division (Carabelli *et al.*, 2007) and other hormones are known to be involved in shade avoidance responses (Gommers *et al.*, 2013). Currently we have poor understanding of the localization and developmental windows of these hormonal (inter)actions, although it is known that some hormones can have very localized effect (e.g. Savaldi-Goldstein *et al.*, 2007; Bargmann *et al.*, 2013). Furthermore, known negative regulators of shade avoidance may similarly play a tissue-specific and developmental age-dependent role. We showed that *HFR1* expression is induced higher in lamina than in petioles, but that the *hfr1* mutant displays wild-type leaf responses (Fig. S2). This in contrast to *hfr1* seedlings, which are known to show enhanced hypocotyl elongation in low R:FR (Sessa *et al.*, 2005). These findings advocate further unraveling of the shade avoidance signaling network taking into account tissue-specific and developmental-determined signals.

ACKNOWLEDGEMENTS

Funding in the Fankhauser lab comes from the University of Lausanne and the Swiss National Science foundation (FNS 310030B_141181/1 to C.F.). This work was further supported by Kempestiftelserna, the Swedish Governmental Agency for Innovation Systems and the Swedish Research Council to K.L. We are grateful to Tino Dornbush for providing the Matlab script to take leaf measurements and to Séverine Lorrain for the *pif4pif5pif7* mutant. We thank Hiroshi Nozaki for kindly providing PEO-IAA, Peter Quail for the *pif7-1* mutant, Joanne Chory for the *sav3-2* mutant and Miguel Blazquez for the *iaa5iaa6iaa19* and *msg2-1* mutants. The *pAFB1::AFB1-GUS, 35S::AFB1-myc* and *tir/afb* lines were generously provided by Mark Estelle. We thank Hannes Richter from the Lausanne Genome Technology Platform (LGTF) for advice on the QPCR analyses, Roger Granbom for excellent technical assistance, Markus Kohnen for browsing previously published ChIP-seq and transcriptomic datasets and three independent reviewers for their useful comments on the manuscript.

REFERENCES

Andersen SU, Buechel S, Zhao Z, Ljung K, Novák O, Busch W, Schuster C, Lohmann JU. **2008**. Requirement of B2-Type Cyclin-Dependent Kinases for Meristem Integrity in Arabidopsis thaliana. *The Plant Cell* **20**: 88–100.

Andriankaja M, Dhondt S, De Bodt S, Vanhaeren H, Coppens F, De Milde L, Mühlenbock P, Skirycz A, Gonzalez N, Beemster GTS, *et al.* 2012. Exit from proliferation during leaf development in Arabidopsis thaliana: a not-so-gradual process. *Developmental Cell* **22**: 64–78.

Ballaré CL, Scopel AL, S a nchez RA. **1990**. Far-red radiation reflected from adjacent leaves: an early signal of competition in plant canopies. *Science* **247**: 329–332.

Bargmann BOR, Estelle M. **2014**. Auxin perception: in the IAA of the beholder. *Physiologia Plantarum* **151**: 52–61.

Bargmann BOR, Vanneste S, Krouk G, Nawy T, Efroni I, Shani E, Choe G, Friml J, Bergmann DC, Estelle M, *et al.* 2013. A map of cell type-specific auxin responses. *Molecular Systems Biology* **9**: 688.

Bou-Torrent J, Galstyan A, Gallemí M, Cifuentes-Esquivel N, Molina-Contreras MJ, Salla Martret M, Jikumaru Y, Yamaguchi S, Kamiya Y, Martinez-Garcia JF. **2014**. Plant proximity perception dynamically modulates hormone levels and sensitivity in Arabidopsis. *Journal of Experimental Botany* **65**: 2937-2947.

Calderon-Villalobos LI, Lee S, De Oliveira C, Ivetac A, Brandt W, Armitage L, Sheard LB, Tan X, Parry G, Mao H, *et al.* 2012. a combinatorial TIR1/AFB–AUX/IAA co-receptor system for differential sensing of auxin. *Nature Chemical Biology* **8**: 477–485.

Carabelli M, Possenti M, Sessa G, Ciolfi A, Sassi M, Morelli G, Ruberti I. **2007**. Canopy shade causes a rapid and transient arrest in leaf development through auxin-induced cytokinin oxidase activity. *Genes & Development* **21**: 1863–1868.

Casal JJ. **2012**. Shade avoidance. *The Arabidopsis Book* **10**: e0157.

Casal JJ. **2013**. Photoreceptor Signaling Networks in Plant Responses to Shade. *Annual Review of Plant Biology* **64**: 403–427.

Chapman EJ, Greenham K, Castillejo C, Sartor R, Bialy A, Sun T-P, Estelle M. **2012**. Hypocotyl transcriptome reveals auxin regulation of growth-promoting genes through GA-dependent and -independent pathways. *PloS One* **7**: e36210.

Chen Q, Dai X, De-Paoli H, Cheng Y, Takebayashi Y, Kasahara H, Kamiya Y, Zhao Y. **2014**. Auxin overproduction in shoots cannot rescue auxin deficiencies in Arabidopsis roots. *Plant & Cell Physiology* **55**: 1072–1079.

Cosgrove DJ. **2005**. Growth of the plant cell wall. *Nature Reviews Molecular Cell Biology* **6**: 850–861.

de Wit M, Lorrain S, Fankhauser C. **2013**. Auxin-mediated plant architectural changes in response to shade and high temperature. *Physiologia Plantarum* **151**: 13–24.

Del Bianco M, Kepinski S. **2011**. Context, Specificity, and Self-Organization in Auxin Response. *Cold Spring Harbor Perspectives in Biology* **3**: a001578–a001578.

Dharmasiri N, Dharmasiri S, Weijers D, Lechner E, Yamada M, Hobbie L, Ehrismann JS, J u rgens G, Estelle M. **2005**. Plant development is regulated by a

593 family of auxin receptor F box proteins. *Developmental Cell* **9**: 109–119.

594 **Donnelly PM, Bonetta D, Tsukaya H, Dengler RE, Dengler NG**. **1999**. Cell cycling
595 and cell enlargement in developing leaves of Arabidopsis. *Developmental Biology*
596 **215**: 407–419.

597 **Duek PD, Fankhauser C**. **2005**. bHLH class transcription factors take centre stage
598 in phytochrome signalling. *Trends in Plant Science* **10**: 51–54.

599 **Evans ML, Ishikawa H, Estelle MA**. **1994**. Responses of Arabidopsis roots to auxin
600 studied with high temporal resolution: Comparison of wild type and auxin-response
601 mutants. *Planta* **194**: 215–222.

602 **Fankhauser C, Chory J**. **2000**. RSF1, an Arabidopsis locus implicated in
603 phytochrome A signaling. *Plant Physiology* **124**: 39–45.

604 **Franklin KA**. **2008**. Shade avoidance. *New Phytologist* **179**: 930–944.

605 **Franklin KA, Praekelt U, Stoddart WM, Billingham OE, Halliday KJ, Whitelam**
606 **GC**. **2003**. Phytochromes B, D, and E act redundantly to control multiple
607 physiological responses in arabidopsis. *Plant Physiology* **131**: 1340–1346.

608 **Gommers CMM, Visser EJW, Onge KRS, Voesenek LACJ, Pierik R**. **2013**. Shade
609 tolerance: when growing tall is not an option. *Trends in Plant Science* **18**: 65–71.

610 **Guilfoyle TJ, Hagen G**. **2007**. Auxin response factors. *Current Opinion in Plant*
611 *Biology* **10**: 453–460.

612 **Havens KA, Guseman JM, Jang SS, Pierre-Jerome E, Bolten N, Klavins E,**
613 **Nemhauser JL**. **2012**. A Synthetic Approach Reveals Extensive Tunability of Auxin
614 Signaling. *Plant Physiology* **160**: 135–142.

615 **Hersch M, Lorrain S, de Wit M, Trevisan M, Ljung K, Bergmann S, Fankhauser**
616 **C**. **2014**. Light intensity modulates the regulatory network of the shade avoidance
617 response in Arabidopsis. *Proceedings of the National Academy of Sciences of the*
618 *United States of America* **111**: 6515–6520.

619 **Holmes MG, Smith H**. **1975**. The function of phytochrome in plants growing in the
620 natural environment. *Nature* **254**: 512–514.

621 **Hornitschek P, Kohnen MV, Lorrain S, Rougemont J, Ljung K, López-Vidriero I,**
622 **Franco-Zorrilla JEM, Solano R, Trevisan M, Pradervand S, *et al.* 2012**.
623 Phytochrome interacting factors 4 and 5 control seedling growth in changing light
624 conditions by directly controlling auxin signaling. *The Plant Journal* **71**: 699–711.

625 **Hornitschek P, Lorrain S, Zoete V, Michielin O, Fankhauser C**. **2009**. Inhibition of
626 the shade avoidance response by formation of non-DNA binding bHLH heterodimers.
627 *EMBO Journal* **28**: 3893–3902.

628 **Jeong J, Choi G**. **2013**. Phytochrome-interacting factors have both shared and
629 distinct biological roles. *Molecules and Cells* **35**: 371–380.

630 **Keller CP, Stahlberg R, Barkawi LS, Cohen JD**. **2004**. Long-term inhibition by
631 auxin of leaf blade expansion in bean and Arabidopsis. *Plant Physiology* **134**: 1217–
632 1226.

633 **Keller MM, Jaillais Y, Pedmale UV, Moreno JE, Chory J, Ballaré CL**. **2011**.
634 Cryptochrome 1 and phytochrome B control shade-avoidance responses in
635 Arabidopsis via partially independent hormonal cascades. *The Plant Journal* **67**:
636 195–207.

637 **Keuskamp DH, Pollmann S, Voesenek LACJ, Peeters AJM, Pierik R**. **2010**. Auxin
638 transport through PIN-FORMED 3 (PIN3) controls shade avoidance and fitness
639 during competition. *Proceedings of the National Academy of Sciences of the United*
640 *States of America* **107**: 22740–22744.

641 **Keuskamp DH, Sasidharan R, Vos I, Peeters AJM, Voesenek LACJ, Pierik R**.
642 **2011**. Blue-light-mediated shade avoidance requires combined auxin and
643 brassinosteroid action in Arabidopsis seedlings. *The Plant Journal* **67**: 208–217.

644 **Kieffer M, Neve J, Kepinski S**. **2010**. Defining auxin response contexts in plant
645 development. *Current Opinion in Plant Biology* **13**: 12–20.

646 **Kozuka T, Kobayashi J, Horiguchi G, Demura T, Sakakibara H, Tsukaya H,**
647 **Nagatani A**. **2010**. Involvement of auxin and brassinosteroid in the regulation of
648 petiole elongation under the shade. *Plant Physiology* **153**: 1608–1618.

649 **Kramer EM**. **2006**. How far can a molecule of weak acid travel in the apoplast or
650 xylem? *Plant Physiology* **141**: 1233–1236.

651 **Kramer EM, Rutschow HL, Mabie SS**. **2011**. AuxV: a database of auxin transport
652 velocities. *Trends in Plant Science* **16**: 461–463.

653 **Leivar P, Monte E**. **2014**. PIFs: systems integrators in plant development. *The Plant*
654 *Cell* **26**: 56–78.

655 **Leivar P, Monte E, Al-Sady B, Carle C, Storer A, Alonso JM, Ecker JR, Quail PH**.
656 **2008**. The Arabidopsis phytochrome-interacting factor PIF7, together with PIF3 and
657 PIF4, regulates responses to prolonged red light by modulating phyB levels. *The*
658 *Plant Cell* **20**: 337–352.

659 **Leivar P, Tepperman JM, Cohn MM, Monte E, Al-Sady B, Erickson E, Quail PH**.
660 **2012**. Dynamic antagonism between phytochromes and PIF family basic helix-loop-
661 helix factors induces selective reciprocal responses to light and shade in a rapidly
662 responsive transcriptional network in Arabidopsis. *The Plant Cell* **24**: 1398–1419.

663 **Li L, Ljung K, Breton G, Schmitz RJ, Pruneda-Paz J, Cowing-Zitron C, Cole BJ,**
664 **Ivans LJ, Pedmale UV, Jung HS, *et al.* 2012**. Linking photoreceptor excitation to
665 changes in plant architecture. *Genes & Development* **26**: 785–790.

666 **Ljung K, Bhalerao RP, Sandberg G**. **2001**. Sites and homeostatic control of auxin
667 biosynthesis in Arabidopsis during vegetative growth. *The Plant Journal* **28**: 465–
668 474.

669 **Lorrain S, Allen T, Duek PD, Whitelam GC, Fankhauser C**. **2008**. Phytochrome-
670 mediated inhibition of shade avoidance involves degradation of growth-promoting
671 bHLH transcription factors. *The Plant Journal* **53**: 312–323.

672 **Mashiguchi K, Tanaka K, Sakai T, Sugawara S, Kawaide H, Natsume M**. **2011**.
673 The main auxin biosynthesis pathway in Arabidopsis. **108**: 18512–18517.

McLaren JS, Smith H. **1978**. Phytochrome control of the growth and development of Rumex obtusifolius under simulated canopy light environments. *Plant, Cell & Environment* **1**: 61–67.

Mellerowicz EJ, Immerzeel P, Hayashi T. **2008**. Xyloglucan: the molecular muscle of trees. *Annals of Botany* **102**: 659–665.

Moreno JE, Tao Y, Chory J, Ballaré CL. **2009**. Ecological modulation of plant defense via phytochrome control of jasmonate sensitivity. *Proceedings of the National Academy of Sciences of the United States of America* **106**: 4935–4940.

Morgan DC, Smith H. **1978**. The relationship between phytochrome-photoequilibrium and Development in light grown Chenopodium album L. *Planta* **142**: 187–193.

Morgan DC, O'Brien T, Smith H. **1980**. Rapid photomodulation of stem extension in light-grown Sinapis alba L. - Studies on kinetics, site of perception and photoreceptor. *Planta* **150**: 95–101.

Nagatani A, Chory J, Furuya M. **1991**. Phytochrome B Is not detectable in the hy3 mutant of Arabidopsis, which is deficient in responding to end-of-day far-red light treatments. *Plant & Cell Physiology* **32**: 1119–1122.

Navarro L, Dunoyer P, Jay F, Arnold B, Dharmasiri N, Estelle M, Voinnet O, Jones JDG. **2006**. A plant miRNA contributes to antibacterial resistance by repressing auxin signaling. *Science (New York, N.Y.)* **312**: 436–439.

Nemhauser JL, Hong F, Chory J. **2006**. Different plant hormones regulate similar processes through largely nonoverlapping transcriptional responses. *Cell* **126**: 467–475.

Nozue K, Harmer SL, Maloof JN. **2011**. Genomic analysis of circadian clock-, light-, and growth-correlated genes reveals PHYTOCHROME-INTERACTING FACTOR5 as a modulator of auxin signaling in Arabidopsis. *Plant Physiology* **156**: 357–372.

Oh E, Kang H, Yamaguchi S, Park J, Lee D, Kamiya Y, Choi G. **2009**. Genome-wide analysis of genes targeted by PHYTOCHROME INTERACTING FACTOR 3-LIKE5 during seed germination in Arabidopsis. *The Plant Cell* **21**: 403–419.

Oh E, Zhu J-Y, Wang Z-Y. **2012**. Interaction between BZR1 and PIF4 integrates brassinosteroid and environmental responses. *Nature Cell Biology* **14**: 802–809.

Oh E, Zhu J-Y, Bai M-Y, Arenhart RA, Sun Y, Wang Z-Y. **2014**. Cell elongation is regulated through a central circuit of interacting transcription factors in the Arabidopsis hypocotyl. *eLife* **3**.

Overvoorde PJ, Okushima Y, Alonso JM, Chan A, Chang C, Ecker JR, Hughes B, Liu A, Onodera C, Quach H, *et al.* 2005. Functional genomic analysis of the AUXIN/INDOLE-3-ACETIC ACID gene family members in Arabidopsis thaliana. *The Plant Cell* **17**: 3282–3300.

Parry G, Calderon-Villalobos LI, Prigge M, Peret B, Dharmasiri S, Itoh H, Lechner E, Gray WM, Bennett M, Estelle M. **2009**. Complex regulation of the TIR1/AFB family of auxin receptors. *Proceedings of the National Academy of Sciences* **106**: 22540–22545.

716 **Pencik A, Simonovik B, Petersson SV, Henykova E, Simon S, Greenham K,**
717 **Zhang Y, Kowalczyk M, Estelle M, Zazimalova E, *et al.* 2013**. Regulation of auxin
718 homeostasis and gradients in Arabidopsis roots through the formation of the indole-
719 3-acetic acid catabolite 2-oxindole-3-acetic acid. *The Plant Cell* **25**: 3858–3870.

720 **Perez-Torres C-A, Lopez-Bucio J, Cruz-Ramirez A, Ibarra-Laclette E,**
721 **Dharmasiri S, Estelle M, Herrera-Estrella L**. **2008**. Phosphate availability alters
722 lateral root development in Arabidopsis by modulating auxin sensitivity via a
723 mechanism involving the TIR1 auxin receptor. *The Plant Cell* **20**: 3258–3272.

724 **Pierik R, Djakovic-Petrovic T, Keuskamp DH, de Wit M, Voesenek LACJ**. **2009**.
725 Auxin and Ethylene Regulate Elongation Responses to Neighbor Proximity Signals
726 Independent of Gibberellin and DELLA Proteins in Arabidopsis. *Plant Physiology*
727 **149**: 1701–1712.

728 **Pierre-Jerome E, Moss BL, Nemhauser JL**. **2013**. Tuning the auxin transcriptional
729 response. *Journal of Experimental Botany* **64**: 2557–2563.

730 **Pitaksaringkarn W, Matsuoka K, Asahina M, Miura K, Sage-Ono K, Ono M,**
731 **Yokoyama R, Nishitani K, Ishii T, Iwai H, *et al.* 2014**. XTH20 and XTH19 regulated
732 by ANAC071 under auxin flow are involved in cell proliferation in incised Arabidopsis
733 inflorescence stems. *The Plant Journal*: n/a–n/a.

734 **Procko C, Crenshaw CM, Ljung K, Noel JP, Chory J**. **2014**. Cotyledon-Generated
735 Auxin Is Required for Shade-Induced Hypocotyl Growth in Brassica rapa. *Plant*
736 *Physiology* **165**: 1285–1301.

737 **Rademacher EH, Moller B, Lokerse AS, Llavata-Peris CI, van den Berg W,**
738 **Weijers D**. **2011**. A cellular expression map of the Arabidopsis AUXIN RESPONSE
739 FACTOR gene family. *The Plant Journal* **68**: 597–606.

740 **Reed JW, Nagpal P, Poole DS, Furuya M, Chory J**. **1993**. Mutations in the gene for
741 the red/far-red light receptor phytochrome B alter cell elongation and physiological
742 responses throughout arabidopsis development. *Plant Cell* **5**: 147–157.

743 **Rose JKC, Braam J, Fry SC, Nishitani K**. **2002**. The XTH family of enzymes
744 involved in xyloglucan endotransglucosylation and endohydrolysis: current
745 perspectives and a new unifying nomenclature. *Plant & Cell Physiology* **43**: 1421–
746 1435.

747 **Sakamoto K, Nagatani A**. **1996**. Nuclear localization activity of phytochrome B. *The*
748 *Plant Journal* **10**: 859–868.

749 **Sasidharan R, Chinnappa CC, Staal M, Elzenga JTM, Yokoyama R, Nishitani K,**
750 **Voesenek LACJ, Pierik R**. **2010**. Light quality-mediated petiole elongation in
751 Arabidopsis during shade avoidance involves cell wall modification by xyloglucan
752 endotransglucosylase/hydrolases. *Plant Physiology* **154**: 978–990.

753 **Sasidharan R, Keuskamp DH, Kooke R, Voesenek LACJ, Pierik R**. **2014**.
754 Interactions between auxin, microtubules and XTHs mediate green shade-induced
755 petiole elongation in Arabidopsis (E Huq, Ed.). *PloS One* **9**: e90587.

756 **Savaldi-Goldstein S, Peto C, Chory J**. **2007**. The epidermis both drives and
757 restricts plant shoot growth. *Nature* **446**: 199–202.

Sessa G, Carabelli M, Sassi M, Ciolfi A, Possenti M, Mittempergher F, Becker J, Morelli G, Ruberti I. **2005**. A dynamic balance between gene activation and repression regulates the shade avoidance response in Arabidopsis. *Genes & Development* **19**: 2811–2815.

Smith H, Holmes MG. **1977**. THE FUNCTION OF PHYTOCHROME IN THE NATURAL ENVIRONMENT?III. MEASUREMENT AND CALCULATION OF PHYTOCHROME PHOTOEQUILIBRIA. *Photochemistry and Photobiology* **25**: 547–550.

Steindler C, Matteucci A, Sessa G, Weimar T, Ohgishi M, Aoyama T, Morelli G, Ruberti I. **1999**. Shade avoidance responses are mediated by the ATHB-2 HD-Zip protein, a negative regulator of gene expression. *Development* **126**: 4235–4245.

Swarup R, Péret B. **2012**. AUX/LAX family of auxin influx carriers-an overview. *Frontiers in Plant Science* **3**: 225.

Takeda T, Furuta Y, Awano T, Mizuno K, Mitsuishi Y, Hayashi T. **2002**. Suppression and acceleration of cell elongation by integration of xyloglucans in pea stem segments. *Proceedings of the National Academy of Sciences of the United States of America* **99**: 9055–9060.

Tao Y, Ferrer JL, Ljung K, Pojer F, Hong F, Long JA, Li L, Moreno JE, Bowman ME, Ivans LJ, *et al.* 2008. Rapid synthesis of auxin via a new tryptophan-dependent pathway is required for shade avoidance in plants. *Cell* **133**: 164–176.

Tatematsu K, Kumagai S, Muto H, Sato A, Watahiki MK, Harper RM, Liscum E, Yamamoto KT. **2004**. MASSUGU2 encodes Aux/IAA19, an auxin-regulated protein that functions together with the transcriptional activator NPH4/ARF7 to regulate differential growth responses of hypocotyl and formation of lateral roots in Arabidopsis thaliana. *The Plant Cell* **16**: 379–393.

Vernoux T, Brunoud G, Farcot E, Morin V, Van den Daele H, Legrand J, Oliva M, Das P, Larrieu A, Wells D, *et al.* 2011. The auxin signalling network translates dynamic input into robust patterning at the shoot apex. *Molecular Systems Biology* **7**: 508.

Vidal EA, Moyano TC, Riveras E, Contreras-Lopez O, Gutierrez RA. **2013**. Systems approaches map regulatory networks downstream of the auxin receptor AFB3 in the nitrate response of Arabidopsis thaliana roots. *Proceedings of the National Academy of Sciences of the United States of America* **110**: 12840–12845.

Vissenberg K. **2005**. Differential expression of AtXTH17, AtXTH18, AtXTH19 and AtXTH20 genes in Arabidopsis roots. Physiological roles in specification in cell wall construction. *Plant & Cell Physiology* **46**: 192–200.

Widman N, Feng S, Jacobsen SE, Pellegrini M. **2014**. Epigenetic differences between shoots and roots in Arabidopsis reveals tissue-specific regulation. *Epigenetics* **9**: 236–242.

Wilson JW, Wilson PMW. **1991**. Effects of auxin concentration on the dimensions and patterns of tracheary elements differentiating in pith explants. *Annals of Botany* **68**: 463–467.

Won C, Shen X, Mashiguchi K, Zheng Z, Dai X, Cheng Y, Kasahara H, Kamiya Y,

Chory J, Zhao Y. **2011**. Conversion of tryptophan to indole-3-acetic acid by TRYPTOPHAN AMINOTRANSFERASES OF ARABIDOPSIS and YUCCAs in Arabidopsis. *Proceedings of the National Academy of Sciences* **108**: 18518–18523.

Yokoyama R, Nishitani K. **2001**. A comprehensive expression analysis of all members of a gene family encoding cell-wall enzymes allowed us to predict cis-regulatory regions involved in cell-wall construction in specific organs of Arabidopsis. *Plant & Cell Physiology* **42**: 1025–1033.

Zazimalova E, Murphy AS, Yang H, Hoyerová K, Hosek P. **2010**. Auxin transporters--why so many? *Cold Spring Harbor Perspectives in Biology* **2**: a001552.

Zhang Y, Mayba O, Pfeiffer A, Shi H, Tepperman JM, Speed TP, Quail PH. **2013**. A quartet of PIF bHLH factors provides a transcriptionally centered signaling hub that regulates seedling morphogenesis through differential expression-patterning of shared target genes in Arabidopsis. *PLoS Genetics* **9**: e1003244.

Zhao Y, Christensen SK, Fankhauser C, Cashman JR, Cohen JD, Weigel D, Chory J. **2001**. A role for flavin monooxygenase-like enzymes in auxin biosynthesis. *Science (New York, N.Y.)* **291**: 306–309.

FIGURE LEGENDS

Figure 1. Petiole and lamina responses of leaf 3 in low R:FR. Petiole length (a), lamina size (b) and relative expression of *PIL1* (c) from leaf 3 (Col-0) over time. Gene expression values were calculated as fold induction relative to petiole sample at t=0. (d,e) Petiole length and lamina size of wild-type (Col-0) and *pif* mutants in high and low R:FR after 3d of treatment. Plants were 15d old at t=0. Error bars represent 2SE, *= p<0.05, Students *t*-test low R:FR vs. high R:FR within genotype. Black bar represents 8h dark period.

Figure 2. Auxin biosynthesis in low R:FR is PIF7-dependent. (a-d) Expression of shade-inducible *YUCCA* genes in petiole and lamina after 2h of control light (high R:FR) or low R:FR. Gene expression values were calculated as fold induction relative to lamina sample at t=0. (e) *YUC8* expression in lamina of wild-type (Col-0) and *pif7* plants over time. Expression values were calculated relative to Col-0 at t=0. (f) Auxin concentration in lamina after 2h of high or low R:FR. Error bars represent 2SE, *= p<0.05, Students *t*-test low R:FR vs. high R:FR within organ (a-d) or genotype (f).

Figure 3. Manipulation of auxin levels mimics low R:FR leaf responses. Petiole length (a,c,e) and lamina size (b,d,f,) of Col-0 plants after 3d of application of 10 μM

IAA or 500 µM L-Kynurenine (Kyn) to the lamina, or 25 µM NPA to the lamina-petiole junction. Error bars represent 2SE, *= p<0.05, Students *t*-test chemical treatment vs. mock application.

Figure 4. Contrasting petiole and lamina responses are not due to different auxin concentration. Basal levels of *YUC8* (a) and *IAA29* (b) in petioles and lamina of 15-day-old plants. Expression values were calculated as fold induction relative to petiole sample. (c) Relative expression of *YUCCA8* in lamina of plants in control light (high R:FR) or low R:FR over time. Vlaues were calculated as fold induction relative to t=0 sample in high R:FR. (d,e) Auxin concentration in petioles and lamina of plants in high or low R:FR over time. Auxin concentration data for Col-0 petioles at t=2h are the same as presented in Figure 2. Error bars represent 2SE, *= p<0.05, Students *t*-test. FW= fresh weight. Black bars represent 8h dark period.

Figure 5. TIR/AFB-mediated auxin perception in low R:FR. *AFB1* expression in petioles (a) and lamina (b) of wild-type (Col-0) and *pif7* after 2h of control light (high R:FR) or low R:FR. Expression values were calculated as fold induction relative to Col-0 sample in high R:FR. (c) Enzyme activity of AFB1-GUS in petioles and lamina of *pAFB1::AFB1-GUS* plants after 24h and 72h of light treatment. (d) Petiole length of *tir1/afb* mutants after 3d of light treatment. (e) Petiole elongation response of Col-0 to low R:FR after application of different concentrations of PEO-IAA. Response was measured as the difference in petiole length between plants in control light and plants in low R:FR after 3d. (f,g) Petiole elongation response to low R:FR in Col-0, *pif7* and *sav3,*after application of 200µM PEO-IAA. Error bars represent 2SE, *= p<0.05, Students *t*-test low R:FR vs. high R:FR within genotype (a,b,d) or organ (c), PEO-IAA vs. mock treatment within genotype in e-g.

Figure 6. Lamina and petiole-specific *XTH* expression. Relative expression of *XTH15* (a) and *XTH19* (b) in petioles and lamina over time in control light (high R:FR) or low R:FR. Expression values were calculated as fold induction relative to petiole sample at t=0. (c,d) Relative expression of *XTH15* in lamina (c) and of *XTH19* in petioles (d) in Col-0 and *pif7*. Expression calculated as fold induction relative to Col-0 sample in high R:FR after 4h of light treatment. Error bars represent 2SE, *= p<0.05, Students *t*-test low R:FR vs. high R:FR within genotype. Black bar represents 8h dark period.

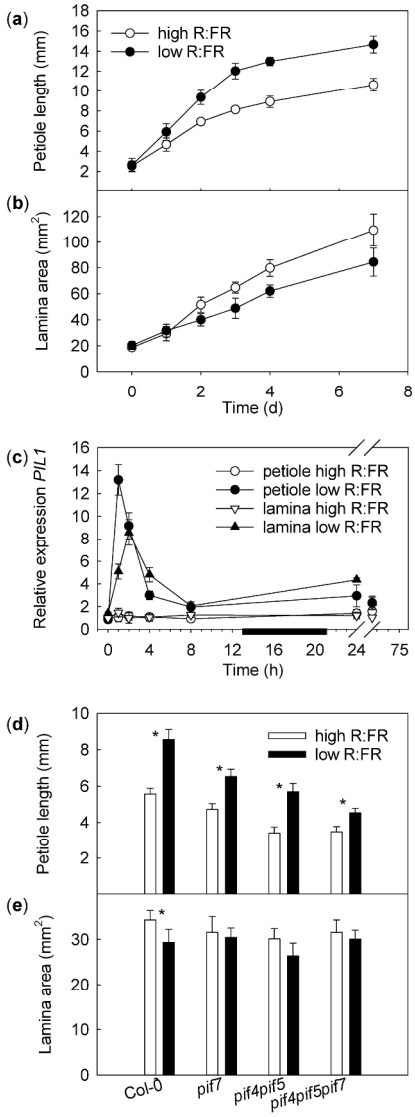

231x425mm (300 x 300 DPI)

Figure 1

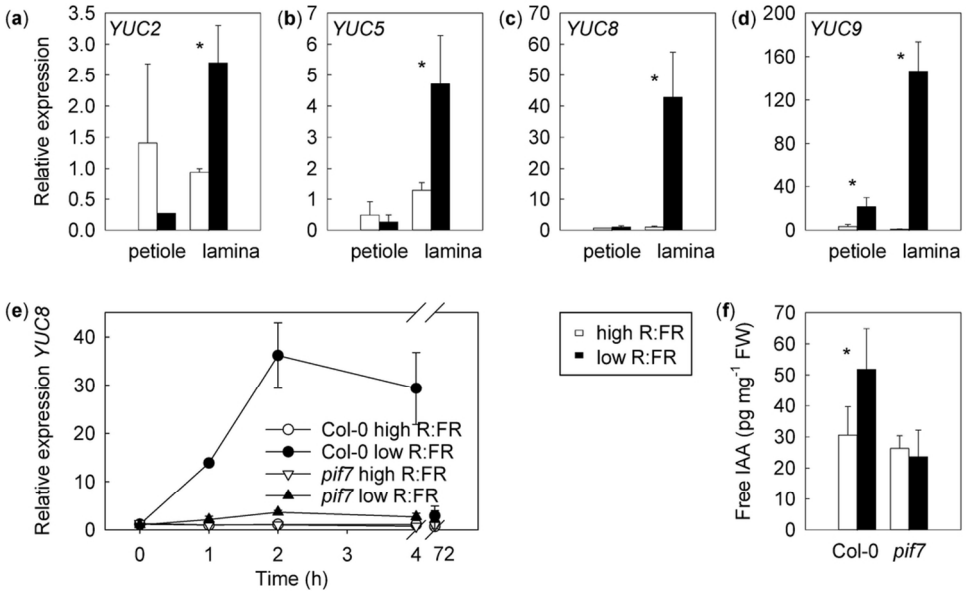

101x63mm (300 x 300 DPI)

Figure 2

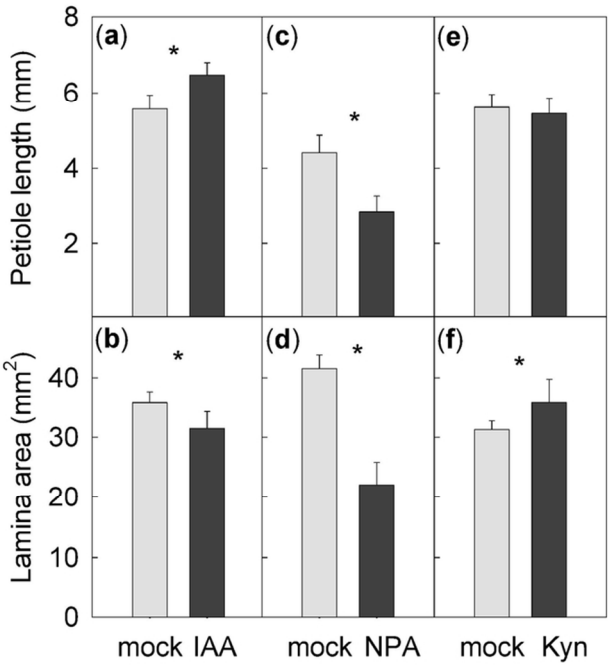

91x72mm (300 x 300 DPI)

Figure 3

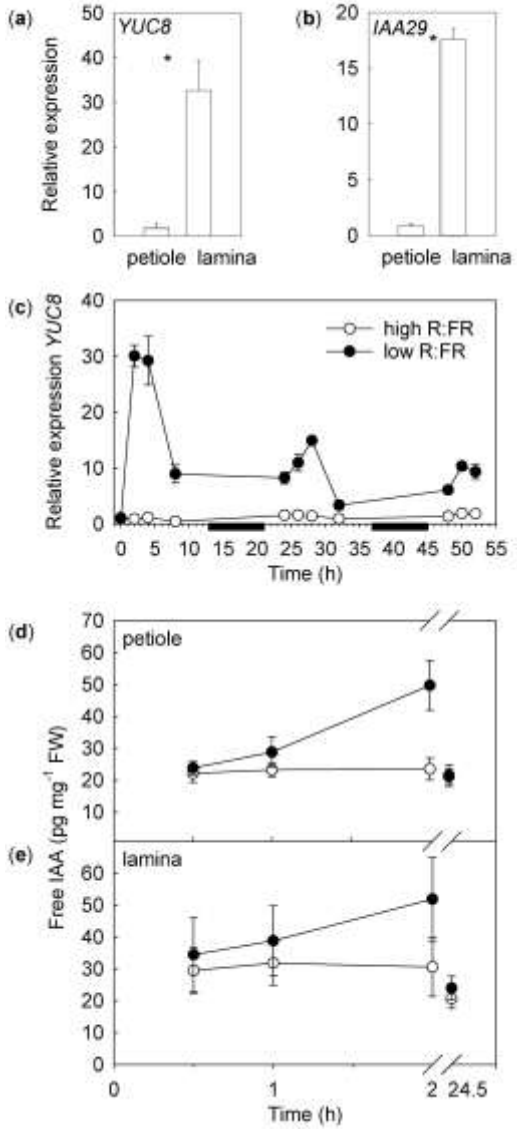

188x419mm (300 x 300 DPI)

Figure 4

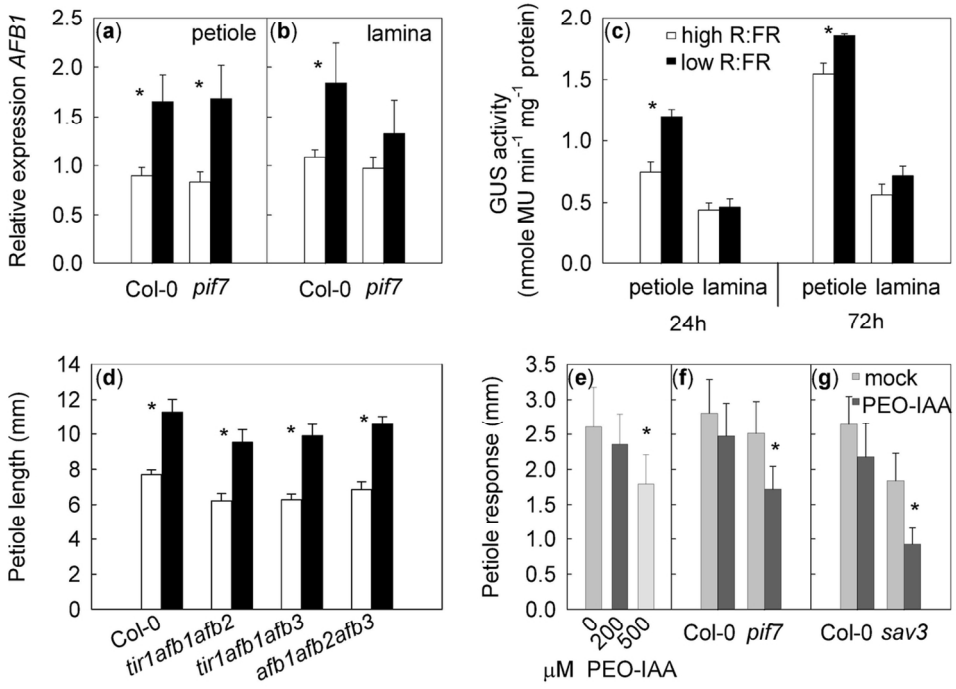

114x91mm (300 x 300 DPI)

Figure 5

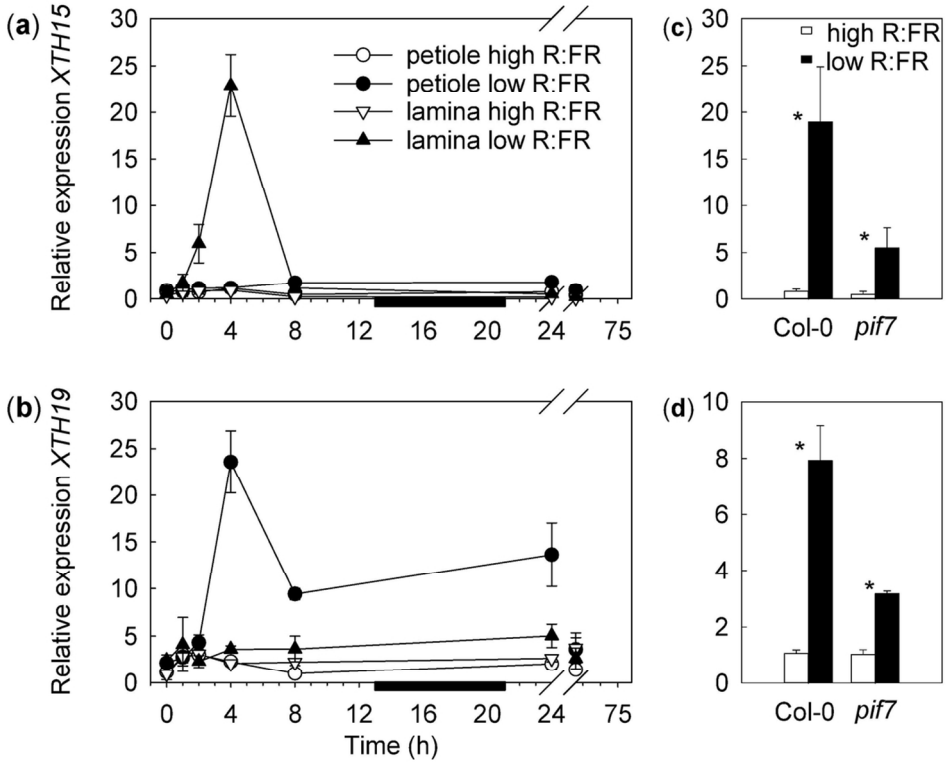

107x92mm (300 x 300 DPI)

Figure 6

New Phytologist **Supporting Information Figs S1–S9, Table S1 and Methods S1**

Article title: **Contrasting growth responses in lamina and petiole during neighbor detection depend on differential auxin responsiveness rather than different auxin levels**

Authors: Mieke de Wit, Karin Ljung and Christian Fankhauser

The following Supporting Information is available for this article:

Fig. S1 Petiole and lamina responses of all leaves in low R : FR.

Fig. S2 Role of HFR1 in shade avoidance phenotype of juvenile leaves.

Fig. S3 Boxplot representation of Fig. 1(d,e).

Fig. S4 Auxin production in the blade leads to growth responses in lamina and petiole.

Fig. S5 Petiole and lamina response to indole-3-acetic acid (IAA) application.

Fig. S6 Expression of *YUC9* in lamina.

Fig. S7 Expression of auxin receptors in leaves.

Fig. S8 Low R : FR-induced petiole elongation in (co)receptor mutants.

Fig. S9 *PIF7* expression in petioles and lamina.

Table S1 Primer sequences used for real time reverse transcriptase (RT)-PCR.

Method S1 Matlab script for petiole length and lamina area analysis.

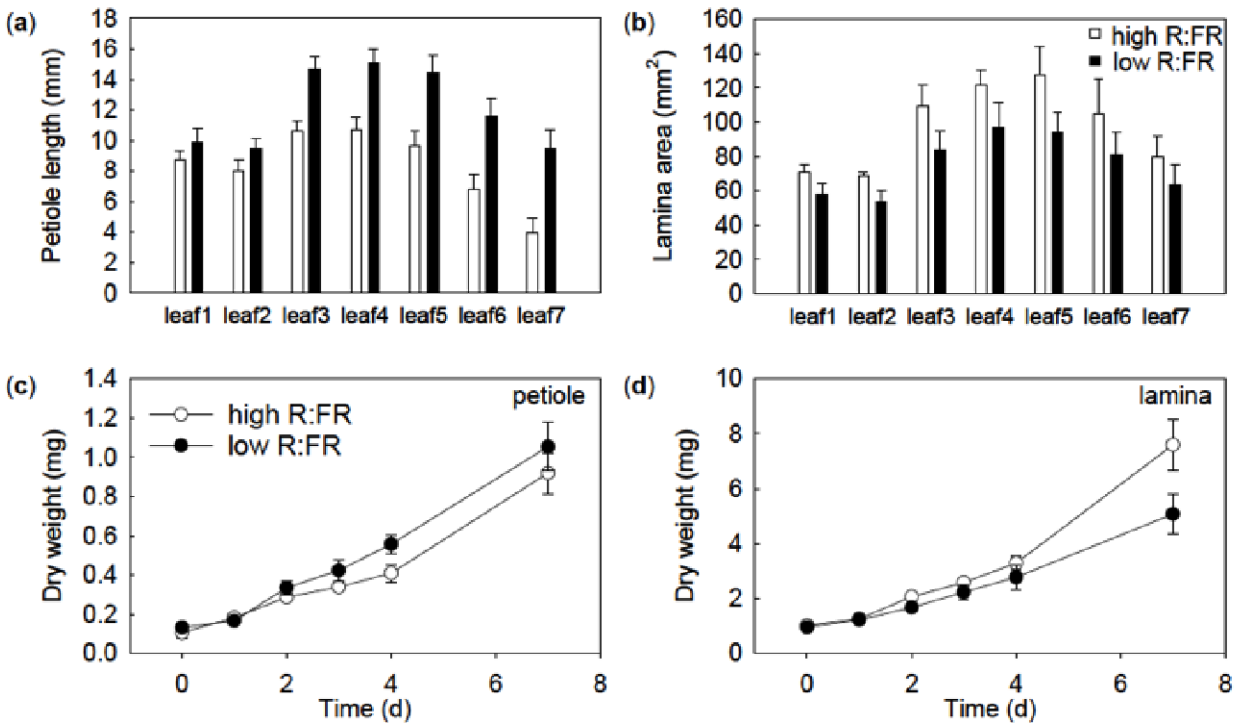

Fig. S1 Petiole and lamina responses of all leaves in low R : FR. (a) Petiole length, (b) lamina size and biomass accumulation of (c) petioles and (d) lamina of all leaves over 7 d of low R : FR treatment. For DWs, petioles and lamina of all leaves per plant were pooled. Plants were 15 d old at t = 0. Error bars represent ± 2 SE.

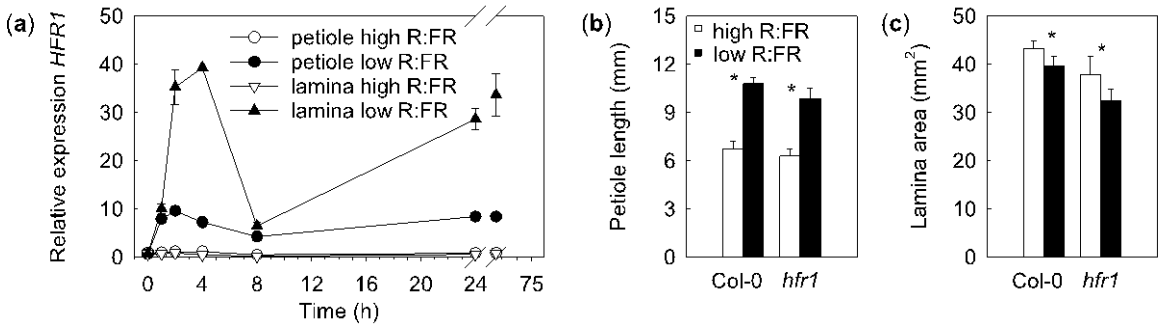

Fig. S2 Role of HFR1 in shade avoidance phenotype of juvenile leaves. (a) Relative expression of *HFR1* in petioles and lamina over time in control light (high R : FR) or low R : FR. Expression values were calculated as fold induction relative to petiole sample at t = 0. (b) Petiole length and (c) lamina size of Col-0 and *hfr1* in high or low R : FR after 3 d of treatment. Error bars represent ± 2 SE; Students *t*-test high R : FR vs low R : FR within genotype: *, $P < 0.05$.

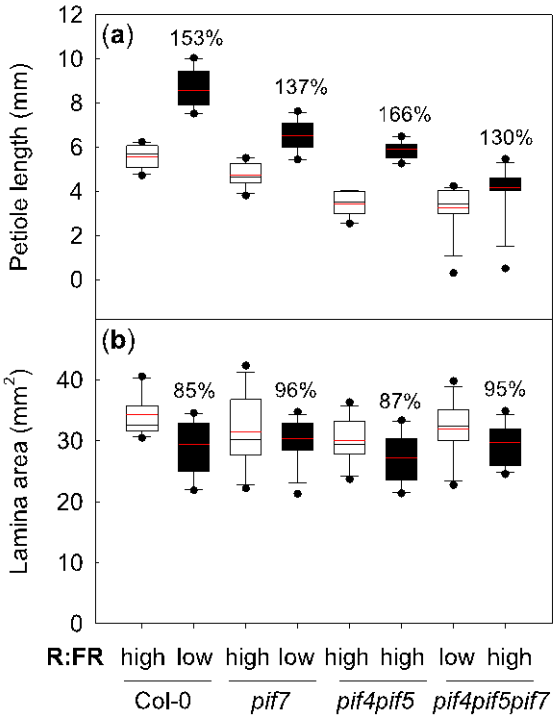

Fig. S3 Boxplot representation of Fig. 1(d,e). (a) Petiole length and (b) lamina size of wild-type (Col-0) and *pif* mutants in high and low R : FR after 3 d of treatment. Tenth, 25th, 75th and 90th percentiles are represented as vertical box with error bars, outliers are shown as black dots. Percentages depicted above boxes represent ratio between high R : FR and low R : FR, red line represents mean.

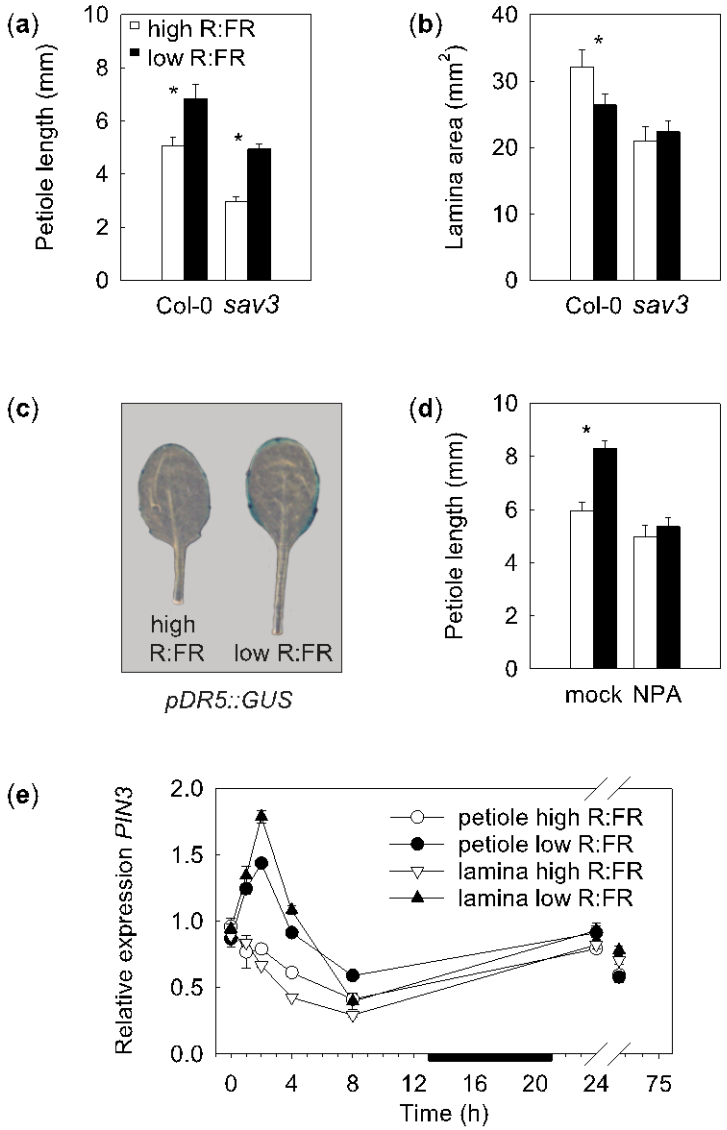

Fig. S4 Auxin production in the blade leads to shade-regulated growth responses in the blade and the petiole. (a) Petiole length and (b) lamina size of Col-0 and *sav3* leaf 3 after 3 d of high or low R : FR. (c) Auxin activity visualized in leaves of *pDR5::GUS* plants after 24 h of high or low R : FR. (d) Petiole length of Col-0 plants in high or low R : FR after 3 d of application of 25 µM naphthylphtalamic acid (NPA) to the lamina-petiole junction. (e) Expression of *PIN3* in petioles and lamina of plants in high or low R : FR over time. Expression values are calculated as fold induction relative to petiole sample at t = 0. Error bars represent ± 2 SE; Students *t*-test low R : FR vs high R : FR within (a, b) genotype or (d) treatment: *, $P < 0.05$.

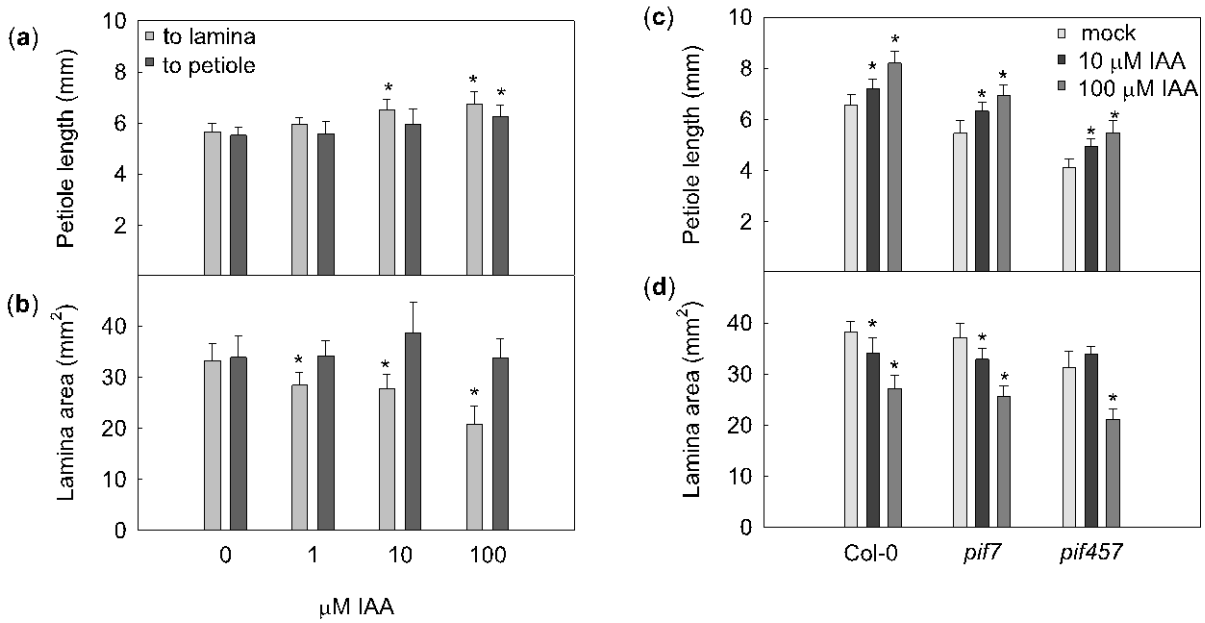

Fig. S5 Petiole and lamina response to indole-3-acetic acid (IAA) application. (a) Petiole length and (b) lamina size of Col-0 plants 3 d after application of different concentrations of IAA either to the lamina (light grey) or application to the petiole (dark grey). (c) Petiole length and (d) lamina size of Col-0 and *pif* mutants after 3 d of application of different concentrations of IAA to leaf 3. Error bars represent + 2 SE; Students *t*-test (a, b) IAA vs mock ('0') application of the same organ or (c, d) IAA vs mock application within genotype: *, $P < 0.05$.

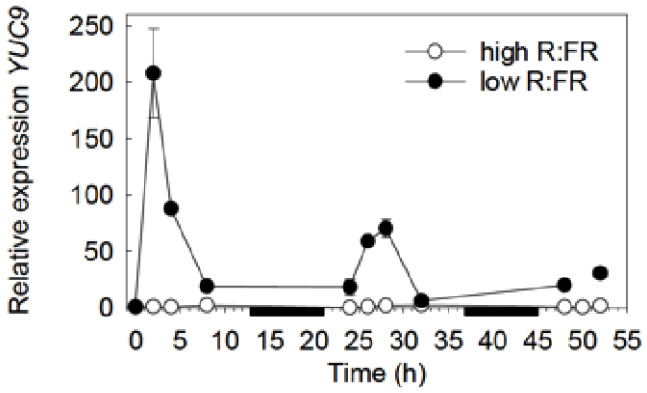

Fig. S6 Expression of *YUC9* in lamina. Relative expression of *YUC9* in lamina of plants in control light (high R : FR) or low R : FR over time. Expression values were calculated as fold induction relative to t = 0 sample in high R : FR. Error bars represent ± 2 SE.

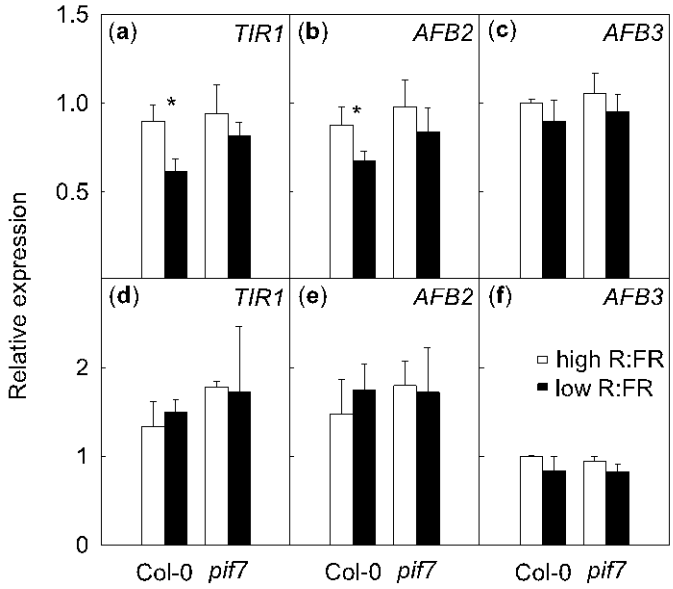

Fig. S7 Expression of auxin receptors in leaves. *TIR1, AFB2* and *AFB3* expression in (a–c) petioles and (d–f) lamina of wild-type (Col-0) and *pif7-1* after 2 h of control light (high R : FR) or low R : FR. Expression values were calculated as fold induction relative to Col-0 sample in high R : FR. Error bars represent + 2 SE; Students *t*-test low R : FR vs high R : FR within genotype: *, $P < 0.05$.

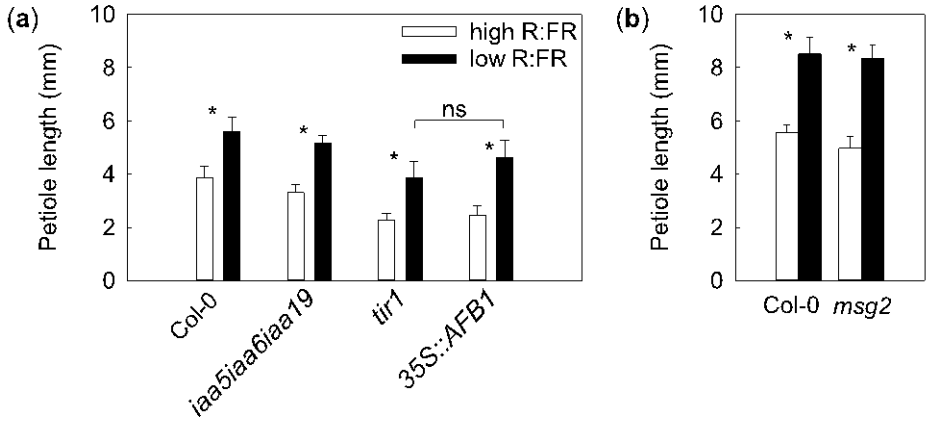

Fig. S8 Low R : FR-induced petiole elongation in (co)receptor mutants. (a) Petiole length of Col-0, the triple mutant *iaa5iaa6iaa19,* the *AFB1* overexpressor *35S::AFB1* in *tir1* background and (b) the dominant IAA19 mutant *msg2* after 3 d of high or low R : FR. Error bars represent + 2 SE; Students *t*-test low R : FR vs high R : FR within genotype: *, $P < 0.05$; ns, not significant.

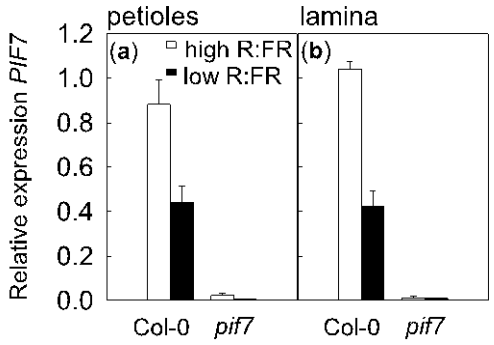

Fig. S9 *PIF7* expression in petioles and lamina. Expression values are calculated as fold induction relative to Col-0 high R : FR sample. Ct values for Col-0 high R : FR were around 22 in petioles and 21 in lamina. Error bars represent + 2 SE.

Table S1. Primer sequences used for Real Time RT-PCR

gene	primer	sequence 5' → 3'
PIL1	F	AAATTGCTCTCAGCCATTCGTGG
	R	TTCTAAGTTTGAGGCGGACGCAG
HFR1	F	GATGCGTAAGCTACAGCAACTCGT
	R	AGAACCGAAACCTTGTCCGTCTTG
YUC2	F	AACTCCGGGATGGAAGTTTG
	R	CCCGAAAGTCGATATACCTAGC
YUC5	F	TGGAGCTAGTAGACGGTCAG
	R	GAAACGGCGATTTCGGGAAC
YUC8	F	GGCGGCTTGTCTCCATGAAC
	R	GATGAACTGACGCTTCGTCG
YUC9	F	GCTAACCACAATGCAATTAC
	R	CATCACTGAGATTCCAAATG
IAA29	F	CTTCCAAGGGAAAGAGGGTGA
	R	TTCCGCAAAGATCTTCCATGTAAC
AFB1	F	GAGCTTCTTAGGCGATGCTC
	R	TCAGTTCTCGCAGTTCCTTG
AFB2	F	AGTCTTGAGCTGCTTTCTCG
	R	GCAAGTGTCTGGGAAACAAC
AFB3	F	GGGTTTACCACTGATGGCTTAG
	R	AGCAGCAACATTGGTCTC
TIR1	F	CTGGGTGCTTGACTACATCG
	R	AAAGGCTCGGACGGAAAC
XTH15	F	CGGCTTGCACAGCCTCTT
	R	TCGGTTGCCACTTGCAATT
XTH19	F	AGTCACGTGGAGTCCCATTC
	R	AATTTGCGGGACAAACTGAC
PIN3	F	AATCGCTTGTGGGAATTCAG
	R	ACAAAGGGCACAATTCCTTG
PIF7	F	AAAGGAGACGGCGTGATAGG
	R	GTGGCAAGTTGGCTCTTAGG

Methods S1 Matlab script for petiole length and lamina area analysis.

As used in Matlab version R2011b, on scanned images of 600 dpi.

```
function D2D_AnalyzePetioleBlade(FolderName)

if margin==0
    FolderName='pathway to folder';
    FileName='';
    A=imread([FolderName '/' FileName]);
else
    FileName=uigetfile({'*.jpg;*.tif;*.png;*.gif','All Image Files';...
        '*.*','All Files' },'Select an image',...
        FolderName)
    A=imread([FolderName '/' FileName]);
end


try
    load([FolderName '/' FileName(1:end-3) 'mat']);
catch
    blade=[];
end



dpi= 600 /2.54;

close all


figure(10),imshow(A)
figure(1),imshow(A)
A=double(A)./255;
count=size(blade,2);

M=[];

% plot already analyzed leaf blades
for i=1:count
    rect=blade(i).rect;

figure(10),rectangle('Position',[rect(1),rect(2),rect(3),rect(4)],'EdgeColor'
,'r')
    figure(10),text(rect(1)+10,rect(2)+40,num2str(i),'Color','r')
    P=blade(i).P_petiole;
    for j=1:size(P,1)
        figure(10),hold on, plot(rect(1)+P(j,1),rect(2)+P(j,3),'ob')

    end
```

```
    M=[M [i, i; blade(count).l_petiole blade(count).A_blade]];

end

if isempty(count)
button='yes';
else
button=questdlg('Select more leaves?', 'Select','Yes','No','Yes');
end

while size(button,2)>2
    count=count+1;

    figure(1)
    [AA,rect]=imcrop(A);
    figure(2),imshow(AA)

    Gray=rgb2gray(AA);

    Red=double(AA(:,:,1));
    Green=double(AA(:,:,2));
    Blue=double(AA(:,:,3));

    %thresholding

    BG=Blue./Green;

    % imshow(BG),impixelinfo

    D=(BG<0.55); %white background
     D=(BG<1); %blue background

    D = imfill(D,'holes');

    % imshow(D.*Gray)
    for j=1:3
        At(:,:,j)=AA(:,:,j).*D;
    end

    figure(3),imshow(At)
    figure(2)
    pause

    button=1;
    x=1;
    P=[];
    while ~isempty(x)

        [x,y] = ginput(1);
        figure(10),hold on, plot(rect(1)+x,rect(2)+y,'ob')
        figure(2),hold on, plot(x,y,'or')
```

```
    if isempty(x)
        figure(2),hold on, plot(P(end,1),P(end,2),'ob')
    else
        P=[P' [x,0,y]']';
    end
end



Pa= diff(P);
% get the rotation angle
 [az,el,~]=cart2sph(Pa(:,1),Pa(:,2),Pa(:,3));

 if az az==pi
    rotation=(-90-el*180/pi);
 else
     rotation=-(-90-el*180/pi);

 end

% Rotate images
Dr=imrotate(D,rotation);
Atr=imrotate(At,rotation);

% make image for selected points
K=zeros(size(D));
for i=1:size(P,1)
K(round(P(i,3)),round(P(i,1)))=1;
end
Kr=imrotate(K,rotation);

% get coordinates of rotated selected points
[xi,yi]=find(Kr==1);
try
Pr(:,1)=yi;
catch
   'e'
end
Pr(:,3)=fliplr(xi')';

Lab= sqrt(sum(Pa.*Pa,2))';
L=sum(Lab)/dpi;

% select pixels above blade/petiole junction point

Bl=Dr(1:xi(1),1:end);

OPIC.ICluster   = bwlabel(Bl(1:end,1:end));

OPIC.stats = regionprops(OPIC.ICluster, ...
    'Area', ...
    'BoundingBox', ...
    'Image' ...
    );
```

```
    PcK=[];
    iC   = find([OPIC.stats.Area] > 500);

    Ds=D2D_CalcOPIC(OPIC,iC);
    figure(5),imshow(Atr)
    figure(5),hold on,imshow(Ds),drawnow
    pause
    Abl=size(find(Ds==1),1)*(1/dpi)^2;

    blade(count).l_petiole=L;
    blade(count).P_petiole=P;
    blade(count).A_blade=Abl;
    blade(count).Ds=Ds;
    blade(count).rect=rect;


    % put a red boundix box


figure(10),rectangle('Position',[rect(1),rect(2),rect(3),rect(4)],'EdgeColor'
,'r')
    figure(10),text(rect(1)+10,rect(2)+40,num2str(count),'Color','r')
    out=[L Abl];

     figure(2), drawnow

    save([FolderName '/' FileName(1:end-3) 'mat'],'blade');

    button=questdlg('Select more leaves?', 'Select','Yes','No','Yes');
    clear AA At Ds D OPIC Gray Dr Atr K Kr P Pr xi yi
    figure(2), close
    figure(3), close
    figure(5), close

    M=[M [count, count; L Abl]];
end


disp(M)


function Ds=D2D_CalcOPIC(OPIC,iC)

cols=size(OPIC.ICluster,2);
rows=size(OPIC.ICluster,1);
Ds=zeros(rows,cols);

for i=iC

    rec=OPIC.stats(i).BoundingBox;
    img=OPIC.stats(i).Image;
    cols_img=size(img,2);
```

```
    rows_img=size(img,1);


    I_left=zeros(rows_img,rec(1));
    I_right=zeros(rows_img,cols-rec(1)-rec(3)+1);

    A=[I_left img I_right];

    I_upper=zeros(cols,rec(2));
    I_lower=zeros(cols,rows -round(rec(2))-rec(4)+1);

    A= [I_upper A' I_lower]';

    Ds=Ds+A;
end


return
```